Hydrogen Bonding and π-Stacking Interactions as Organizing Elements in Lariat Ethers Containing Nucleotide Bases

Otto F. Schall and George W. Gokel*

Bioorganic Chemistry Program and Department of Molecular Biology & Pharmacology, Washington University School of Medicine, Campus Box 8103, 660 S. Euclid Avenue, St. Louis, Missouri 63110

Received November 3, 1995[⊗]

Two new bibracchial lariat ethers have been prepared as flexible model systems for nucleotide H-bonding and π-stacking interactions. In both compounds, nucleotide bases terminate side arms attached at the nitrogen atoms of a diaza-18-crown-6 macroring. Each side arm is terminated by one or more nucleotide bases. The unsymmetrical structure is ade-CH_2CH_2<N18N>$CH_2CH_2CH_2$-thy-CH_2CH_2-ade (A−O−T−A). The symmetrical compound is ade-CH_2CH_2-thy-CH_2CH_2-CH_2<N18N>$CH_2CH_2CH_2$-thy-CH_2CH_2-ade (A−T−O−T−A). NMR studies show that the thy−ade side arm organizes by π-stacking in both A−O−T−A and A−T−O−T−A. Both compounds exhibit hydrogen bonding between the stacked base pair and the opposite adenine. A−O−T−A exhibits a stronger interaction resulting from the enforced interplay of noncovalent forces, as evidenced by one- and two-dimensional NMR experiments. This compound also presented the opportunity to detect and examine single hydrogen-bonded interactions between two adenine bases. The effects of conformational rigidity, side arm orientation, metal ion complexation, and variations in solvent were assessed for both compounds. The results presented here indicate that an increase in the medium's dielectric constant or complexation of metal cations appear to modulate the interplay between hydrogen bonding and stacking interactions.

Introduction

Although the amino acid sequence defines any given protein, it is the noncovalent forces that ultimately facilitate function.[1] We have been interested for some years in developing systems that have "flexible frameworks" but which function as the result of the same noncovalent forces that are crucial in determining the secondary-quaternary structure of *inter alia* nucleic acids, proteins, and enzymes. Among these forces, hydrogen bonding[2] is probably the best studied, but π-stacking,[3] Coulombic interactions, and hydrophobic forces[4] are all known to be of great consequence. Nearly 500 solid state structures of large biomolecules have been obtained, and much solution work has also been reported which reveals structural detail. Site-directed mutagenesis offers the prospect of selective, location-specific structural alteration, but the consequence of a single amino acid change may be magnified by the overall structural complexity of the system under study. For these reasons, bioorganic model systems[5] continue to offer the best access to controlled and subtle structural variations whose effects can be assessed and comprehended at the molecular level. Many model systems have been developed that may resemble DNA or may have incorporated deliberate features so that specific issues can be addressed. The recent crystal structure of a self-associating DNA heptamer that forms base quadruplets and exhibits a variety of intramolecular H-bond arrays is but one example.[6]

We have recently reported the results of an effort to assess hydrogen-bond-induced molecular organization using adenine−thymine base pairs as the ordering element in an otherwise flexible array.[7] In these systems, side arms attached to crown ethers were terminated by two adenines, two thymines, or one of each. In the course of these studies, we designed, prepared, and studied by a variety of methods the extent and modes of association exhibited by these systems. In particular, we were able to assess the extent of aggregation stabilized by H-bond formation and whether or not there was a preference for Watson−Crick or Hoogsteen interactions in this otherwise flexible molecular ensemble. In this report, we present the results of detailed one- and two-dimensional NMR studies and molecular modeling on the two novel and complex molecular systems A−O−T−A and A−T−O−T−A. The combination of these new compounds and the various structural studies that have been conducted afford what we believe to be a clear indication of simultaneous interplay between hydrogen bonding and π-stacking. We have used these results to understand the influence of these interactions on conformation.

[⊗] Abstract published in *Advance ACS Abstracts,* February 1, 1996.

(1) (a) Creighton, T. E.; *Proteins: Structures and MolecularProperties,* 2nd ed.; W. H. Freeman: New York, 1993. (b) Stickle, D. F.; Presta, L. G.; Dill, K. A.; Rose, G. D. *J. Mol. Biol.* **1992**, *226*, 1143. (c) Williams, D. H. *Aldrichim. Acta* **1991**, *24*, 71. (d) Hamilton, A. D. Hydrogen Bonding in Biological and Artificial Molecular Recognition. *Advances in Supramolecular Chemistry*; JAI: Greenwich, CT, 1990; Vol. 1.

(2) Jeffrey, G. A.; Saenger, W. *Hydrogen Bonding in Biological Structures*; Springer Verlag: Berlin, 1991.

(3) (a) Hunter, C. A. *Chem. Soc. Rev.* **1994**, 101. (b) Hunter, C. A.; Sanders, J. K. M. *J. Am. Chem. Soc.* **1990**, *112*, 5525. (c) Burley, S. K.; Petsko, G. A. *Science* **1985**, *229*, 23. (d) Kumar, N. V.; Govil, G. The Role of Stacking in Protein: Nucleic Acid Interactions. In *Conformation in Biology*; Srinivasan, R., Sarma, R. H., Eds.; Adenine Press: New York, 1983.

(4) Israelachvili, J. N. *Intermolecular and Surface Forces,* 2nd ed.; Academic Press: New York, 1991.

(5) (a) Inouye, M.; Konishi, T.; Kakuzo, I. *J. Am. Chem. Soc.* **1993**, *115*, 8091. (b) Galan, A.; De Mendoza, J.; Toiron, C.; Bruix, M.; Deslongchamps, G.; Rebek, J., Jr. *J. Am. Chem. Soc.* **1991**, *113*, 9424. (c) Tjivikua, T.; Deslongchamps, G.; Rebek, J., Jr. *J. Am. Chem. Soc.* **1990**, *112*, 8408. (d) Dugas, H. *Bioorganic Chemistry*, 2nd ed.; Springer-Verlag: Berlin, 1989. (e) Goswani, S.; Hamilton, A. D. *J. Am. Chem. Soc.* **1989**, *111*, 3425. (f) Jeong, K. S.; Rebek, J., Jr. *J. Am. Chem. Soc.* **1988**, *110*, 3327. (g) Rebek, J., Jr.; Askew, B.; Bellester, P.; Buhr, S. J.; Nemeth, D.; Williams, K. *J. Am. Chem. Soc.* **1987**, *109*, 5033.

(6) Leonard, G. A.; Zhang, S.; Peterson, M. R.; Harrop, S. J.; Helliwell, J. R.; Cruse, W. B. T.; Langlois d'Estaintot, B.; Kennard, O.; Brown, T.; Hunter, W. N. *Structure* **1995**, *3*, 335.

(7) (a) Schall, O. F.; Gokel, G. W. *J. Chem. Soc., Chem. Commun.* **1992**, 748. (b) Schall, O. F.; Gokel, G. W. *J. Am. Chem. Soc.* **1994**, *116*, 6089.

0022-3263/96/1961-1449$12.00/0

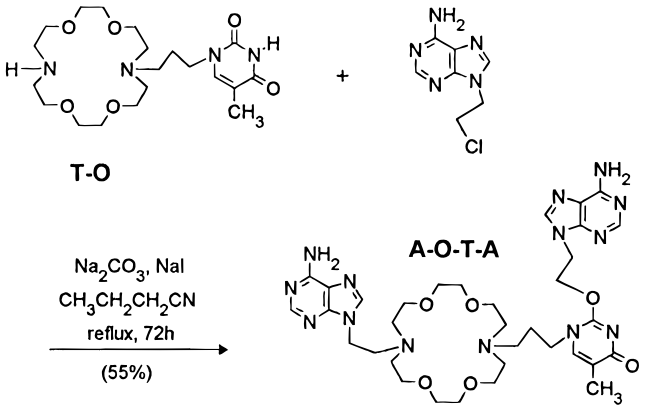

Figure 1. Synthesis of the unsymmetrical monomer, A−O−T−A.

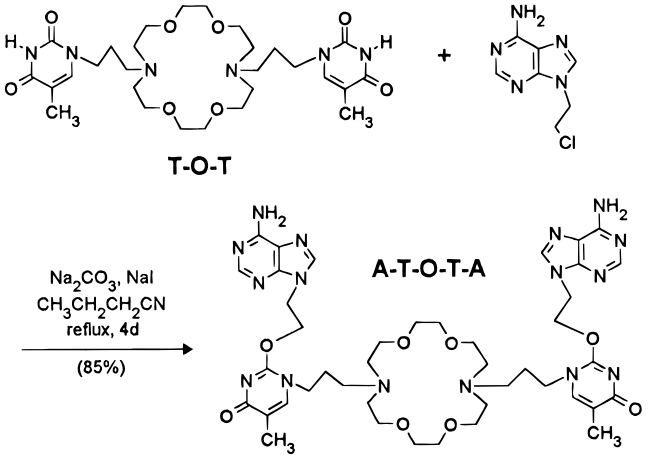

Figure 2. Synthesis of the symmetrical monomer, A−T−O−T−A.

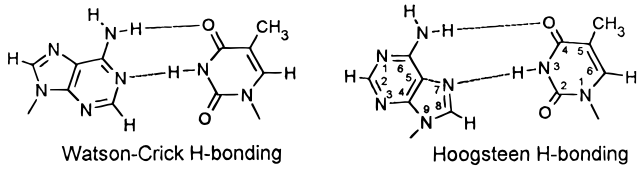

Figure 3. Watson−Crick and Hoogsteen hydrogen bonding modes between adenine and thymine and the numbering system for the purine and pyrimidine rings.

Results and Discussion

Shorthand Nomenclature. The compounds reported herein are derivatives of 4,13-diaza-18-crown-6 which we represent as <N18N>[8] or when structure names are highly abbreviated, simply as "O". The $(CH_2)_n$ side chains are represented only by a hyphen, and the nucleotide bases which are normally designated by the standard abbreviations of ade, thy, gua, and cyt are represented in the structures as A, T, G, and C. Thus, ade-CH_2CH_2-CH_2-<N18N>-$CH_2CH_2CH_2$-ade reduces to A−O−A.

Design And Syntheses. Two compounds were of special interest to us in the present study. In our previous work with A−O−A and T−O−T, a single nucleotide base was attached to each side arm. Interactions of the purines and pyrimidines could occur by H-bonding either inter- or intramolecularly. Stacking interactions were more difficult to assess because the side arms were attached to opposite ends of the macrorings and could not necessarily achieve the most favorable stacking geometry. Attaching both adenine and thymine to each other and to the same side arm offered an opportunity to assess the combination of π-stacking and H-bonding in these generally flexible systems. Although in these molecules the pyrimidine ring was not formally thymine, these models provided a framework to study hydrogen bonding and stacking potential, their effects on local conformation, and their modulation in a DNA baselike environment.

Two diaza-18-crown-6 derivatives were prepared for use in the present study. In both cases, an ethylene or propylene chain was terminated in one or more nucleotide bases. The single-armed derivative of 4,13-diaza-18-crown-6, thy$CH_2CH_2CH_2$ <N18N>H or T−O, was obtained from the previously reported[7b] preparation of T−O−T. Reaction of T−O with 9-(2−chloroethyl)adenine (Na_2CO_3, NaI, Pr-CN, reflux for 72 h) as shown in Figure 1 afforded A−O−T−A in 55% yield (mp 136−138 °C). The structure of the compound was confirmed in part by DCI mass spectrometry (mw 751, calculated 750.86 g mol^{-1}) and by combustion analyses of it and its $NaBPh_4$ salt.

The crown ether having two "combination" side arms, A−T−O−T−A, was prepared in a single step from T−O−T by reaction as above with 2.2 equiv of 9-(2-chloroethyl)adenine (Na_2CO_3, NaI, PrCN, reflux, 4 d) to afford A−T−O−T−A as a white solid (mp 113−116 °C) in 85% yield. The preparation is shown in Figure 2.

Solution Conformational Studies of A−O−T−A. The attachment of adenine to thymine by an ethyleneoxy (formally ethylene to the thymine urea (C2) oxygen) unit in the side arms of either A−O−T−A or A−T−O−T−A presented the opportunity to assess how these complementary nucleotide bases interact. The short chain connecting T and A is flexible but its length prohibits interaction by either Hoogsteen (involving adenine's N7 as acceptor) or Watson−Crick (involving adenine's N1 as acceptor) H-bonding modes. Thus this system could be used to learn about stacking interactions in each side arm and also to observe crossring side arm interactions involving nucleotide bases on opposite sides of the macrocyclic ring. For the sake of clarity in the subsequent discussion, we show above (Figure 3) the structures of adenine and thymine and the standard numbering system used to designate positions in the nucleotide bases. Both Watson−Crick and Hoogsteen binding modes are illustrated.

The gross orientation of adenine and thymine in the side arms is determined by the fact that adenine-N9 and thymine-O2 are covalently linked. The ethylene chain that bridges these atoms permits some flexibility but the relative orientation remains fixed. Various possibilities for π-stacking by these connected residues are shown in Figure 4. The wavy lines indicate connection to the crown ether residue. Note that thymine is bonded to the macrocyclic ring through N1. The O−C bond from thymine to the 2-adenylethyl chain can be oriented either *syn* or *anti* with respect to it. Further, the thymine ring may prefer to overlap the purine predominantly on its five- or six-membered side.

Positional assignments of NMR resonances and details of the solution structures were obtained by 2D-COSY and NOESY NMR experiments conducted at 400 MHz in $CDCl_3$ (75 mM 2D-COSY and NOESY samples studied at 22 °C are shown, respectively, in Figures 5 and 6). It is interesting to note that, at a concentration of 150 mM,

(8) Hernandez, J. C.; Trafton, J. E.; Gokel, G. W. *Tetrahedron Lett.* **1991**, 6269.

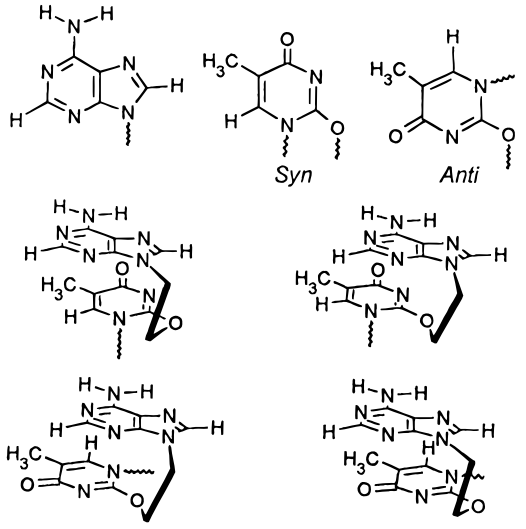

Figure 4. Possible stacking orientations between the adenine and thymine side arm residues.

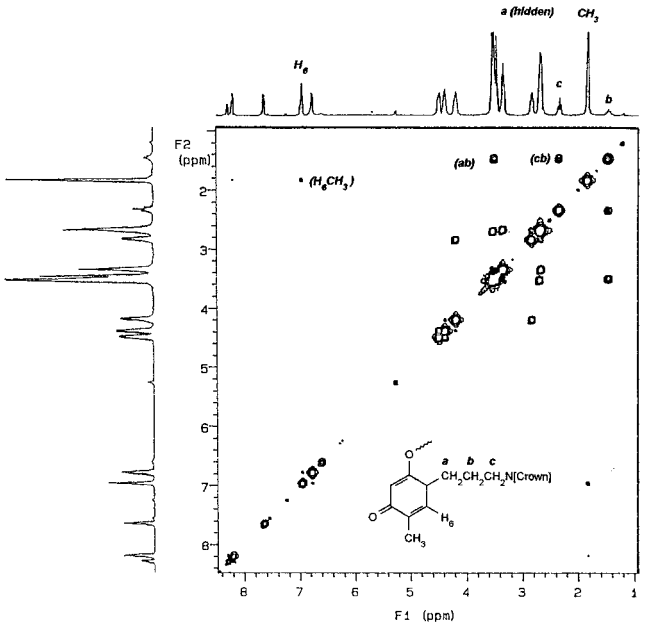

Figure 5. COSY spectrum of A−O−T−A.

the amino resonance observed at 6.818 ppm afforded a considerably sharper signal and was located 0.187 ppm more downfield than the other (6.631 ppm). Upon dilution to 5 mM both amino resonances shifted upfield; however, the shift of the sharper, more downfield resonance was only +0.023 ppm, while the other was nearly 8-fold greater (+0.169 ppm). In addition, some of the resonances assigned to the carbon-bound hydrogens in the adenine and thymine moieties appeared at frequencies significantly different from those in A−O−A and T−O−T relatives,[7b] which were observed at the following positions: A−O−A, C8 = 7.950 ppm; T−O−T, C6 = 7.178 ppm; A−O−T−A, (A)C8 = 8.263 ppm, (AT)C8 = 7.629 ppm, C6 = 6.941 ppm.

Detailed analysis of the spectra was accomplished by constructing CPK molecular models of the various possible conformations, accounting for the observed NOEs, and examining the experimental chemical shifts. In this way, we deduced that in $CDCl_3$ A−O−T−A folds so that π-stacking can occur between ade and thy on the long side arm. In addition, a hydrogen bond forms between

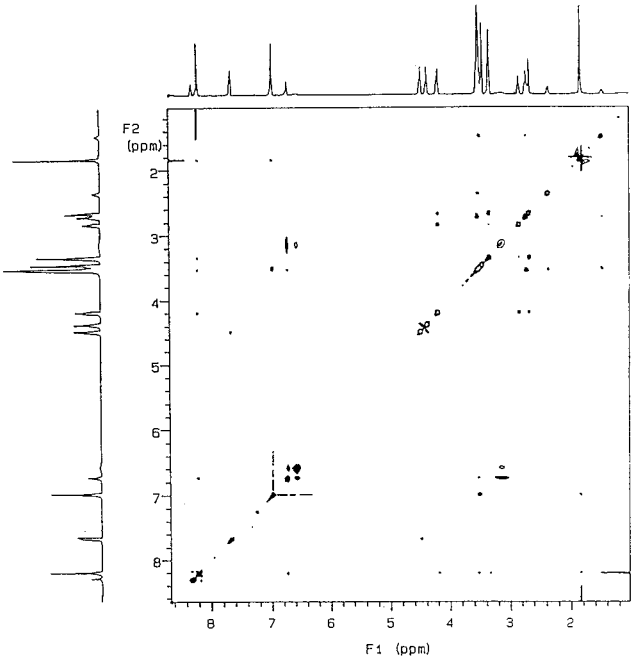

Figure 6. NOESY spectrum of A−O−T−A.

the lone ade from its 6-amino group to N7 in the opposite purine. Upfield positions of the H6 and N1−CH_2 resonances (see Table 2 below) in the pyrimidine ring are consistent with alkylation at O2 rather than O4 and magnetic shielding of H6 and thy-CH_2 by the purine system. The alkylation site is further supported by NOE data and the fact that the C5-CH_3 resonance, which is adjacent to O4, is not shifted comparatively. As shown in Figure 7, thymine stacks with the five-membered ring of adenine (in its own AT side arm). The proposed stacking geometry for this sytem, in which the molecules concerned do not overlap completely, has been observed.[2,3d,9] In base−base and base−aromatic amino acid stacking, heteroatoms such as O and N usually overlap with polarizable regions of the delocalized system. Solid state structures confirm such geometries.[2,3d] In any case, the postulated stacking pattern explains the upfield shifts observed for certain resonances.[10]

The chemical shift data for the amino group resonances of both adenines suggest that these participate in hydrogen bonding. Based upon the spectral data and molecular models, a single H-bond interaction of the Hoogsteen type is most likely. Either Hoogsteen or Watson−Crick H-bonding would bring the A side arm into position to shield C6-H and N1-CH_2 in the pyrimidine ring. Such a conformational approach and shielding from the adenine in the same side arm would account for the upfield shifts observed for these hydrogens. In addition, an interaction of the Hoogsteen type would bring the C8-H in the A side arm near the combined

(9) Saenger, W. *Principles in Nucleic Acid Structure*; Springer-Verlag: New York, 1984.
(10) (a) Williams, N. G.; Williams, L. D.; Shaw, B. R. *J. Am. Chem. Soc.* **1990**, *112*, 829. (b) Smithrud, D. B.; Sanford, E. M.; Chao, L.; Ferguson, S. B.; Carcanague, D. R.; Evanseck, J. D.; Houk, K. N.; Diederich, F. *Pure Appl. Chem.* **1990**, *62*, 2227. (c) Hamilton, A. D.; Little, D. *J. Chem. Soc., Chem. Commun.* **1990**, 297. (d) Lehn, J.-M.; De Mendoza, J.; Galan, A.; Echavarren, A. *J. Am. Chem. Soc.* **1989**, *111*, 4994. (e) Williams, N. G.; Williams, L. D.; Shaw, B. R. *J. Am. Chem. Soc.* **1989**, *111*, 7205. (f) Leonard, N. J. *Acc. Chem. Res.* **1979**, *12*, 423. (g) Leonard, N. J.; Gruber, B. A.; Mutai, J. *J. Am. Chem. Soc.* **1975**, *97*, 4095. (h) Schweizer, M. P.; Broom, A. D.; Ts'o, P. O. P. *J. Am. Chem. Soc.* **1968**, *90*, 1042.

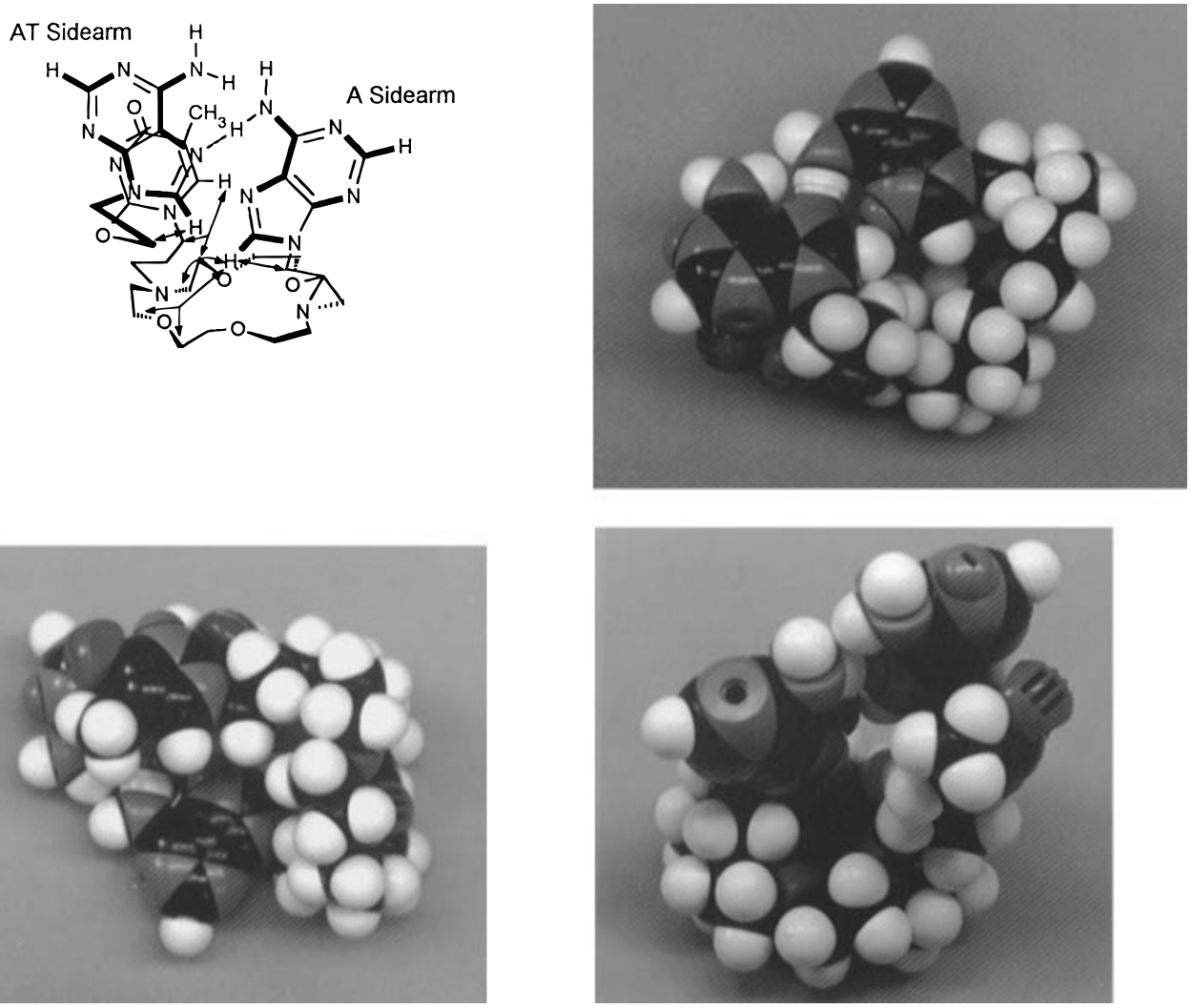

Figure 7. (Top left) Representation of the proposed solution conformation of A−O−T−A. Both adenine rings rest in approximately the same plane. The adenine residue on the left is stacked on the pyrimidine ring system. (Top right) CPK molecular model illustrating the proposed conformation as represented in top left. (Lower left) CPK molecular model of A−O−T−A viewed from the pyrimidine side (opposite to that shown in top right). (Lower right) CPK molecular model of A−O−T−A viewed from above, through the center of the crown ether ring.

deshielding regions of the stacked AT side arm and would also explain its downfield position (8.263 ppm in $CDCl_3$, compared to 7.950 ppm in A−O−A).

All resonance assignments were confirmed by a combination of deuterium replacement of the slightly acidic C8-H's (D_2O solutions, see Experimental Section)[11] and variations in the acquisition time and relaxation delay using one-dimensional ^{1}H-NMR. As a result of these studies, we noted that the C2−H's resonances require longer relaxation periods than do the C8-H's, and that the intensities of both vary with relaxation delay (D1) times.

Molecular Modeling Studies. Many conformations are possible for a molecule as flexibile as A−O−T−A. Two criteria must be met by any postulated structural arrangement: it must be chemically reasonable and it cannot be contradicted by any experimental evidence. Because A−O−T−A involves nucleotide bases, π-stacking and/or H-bonding seemed likely to stabilize any low energy conformation. We therefore subjected several chemically reasonable conformations to energy minimization using the computer program SYBYL. Some of the most likely alternative structures are compared in Figure 8a−d. The conformation inferred from the data discussed above is illustrated in Figure 8a as viewed from the top of the molecule, through the crown ether ring. Its energy was arbitrarily set to 0 kcal/mol (medium dielectric = 4.8).

Figure 8b depicts the view of a structure in which adenine in the A side arm hydrogen bonds to the C4-carbonyl oxygen atom of thymine in a Watson−Crick fashion. This conformation does not accord with our interpretation of the data. Specifically, the downfield position of the C8-H resonance in the A side arm is not expected in this conformation nor are the observed NOEs between this signal and signals arising from hydrogens in the crown ether ring (see Figure 7). In addition, the N−H bond involved in intramolecular H-bonding presents itself to the sp^2 orbitals of the carbonyl oxygen almost perpendicularly. The interaction energy calculated by the program for this conformation was ~1.2 kcal/mol larger than for the structure shown in Figure 8a.

In Figure 8c, the adenine rings are contained in almost orthogonal planes. Although such a conformation would

(11) Chan, S. I.; Schweizer, M. P.; Ts'o, P. O. P.; Helmkamp, G. K. *J. Am. Chem. Soc.* **1964**, *86*, 4182.

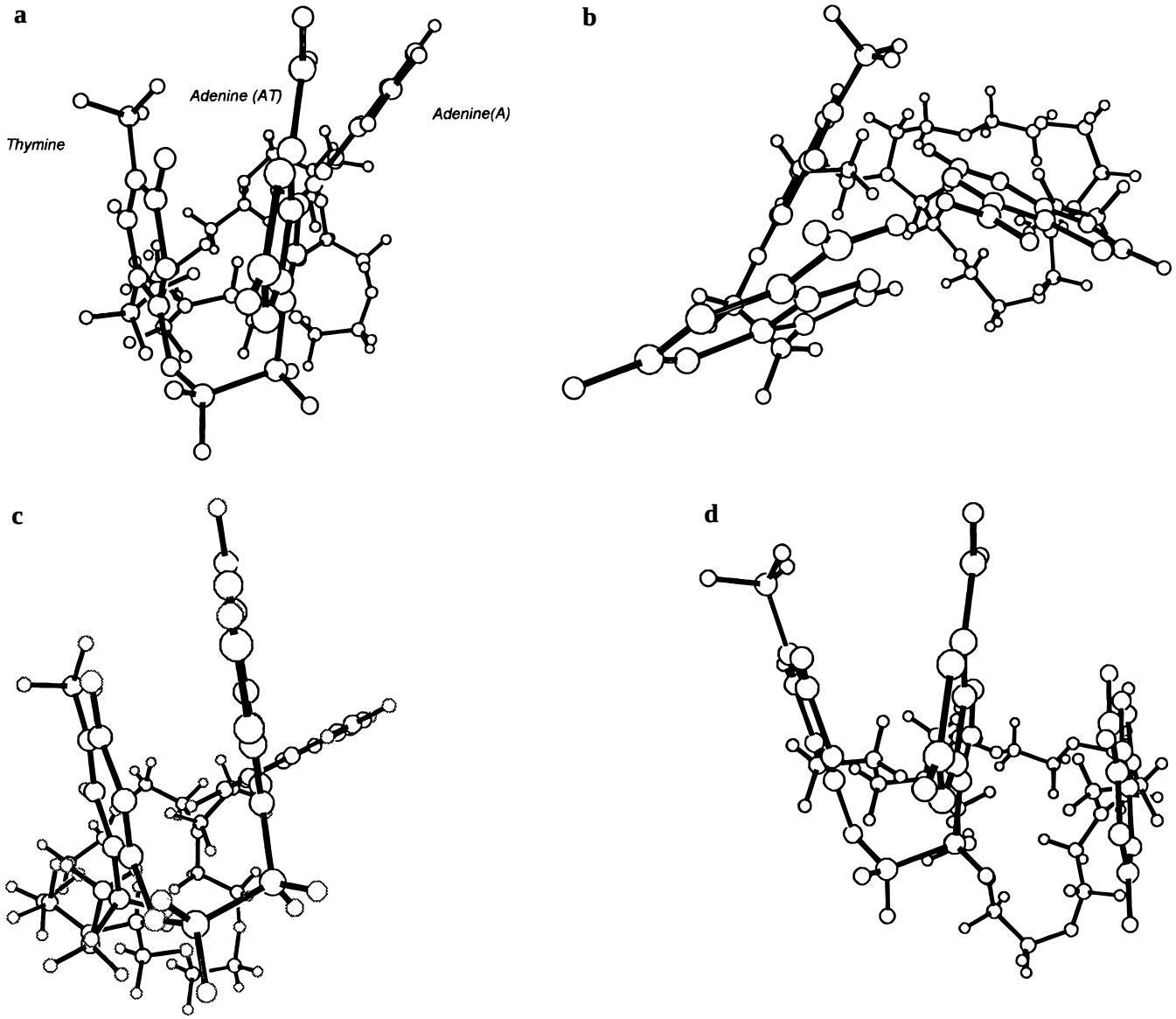

Figure 8. (a) Computer-generated image of the conformation illustrated in Figure 7 (top left) as viewed from the above, through the center of the crown ether ring. (b) Similar view in which the adenine on the A side arm hydrogen bonds to thymine's C4 carbonyl oxygen atom. (c) Computer-generated image showing the two adenine residues contained in approximately orthogonal planes. (d) Illustration of the effect on conformation of an increase in the medium dielectric constant.

support the NMR data and might reduce dipole repulsions between the adenine N−H bonds, no intramolecular hydrogen bond results. The interaction energy calculated for this conformation was ~1.7 kcal/mol higher than that of the conformation displayed in Figure 8a.

Figure 8d illustrates the conformational effect resulting from increasing the medium's dielectric constant from 4.8 ($CHCl_3$ solution) to 37.5 (CH_3CN solution). These dielectric constants were chosen because NMR spectra of these systems are accessible in the corresponding solvents. Compared to the structure shown in Figure 8a, the change in dielectric constant causes the adenine in the A side arm to compromise its H-bond donicity to the AT side arm by assuming a position almost parallel to the second adenine (AT side arm). In this situation, the A side arm is in position to contribute to the overall base-stacking. In addition, the separation between the mean planes of the thymine and adenine residues in the AT side arm increases by approximately 0.3 Å.

Solution Conformation Studies of A−T−O−T−A. In broad outline, the 400 MHz NMR spectrum of A−T−O−T−A is similar to that of A−O−T−A. Shift trends, similar to those observed for A−O−T−A, attributable to π-stacking of the side arms, are evident. The hydrogen-bond-induced organization of the side arms is also apparent. Data are recorded in Table 1 (see below).

Aggregation Behavior of A−O−T−A and A−T−O−T−A. We have previously established the value of vapor pressure osmometry (VPO) in assessing, qualitatively, the extent of aggregation (*e.g.* intermolecular association) of similar DNA base-containing lariat ethers and self-assembling Ni(II) aggregates.[7b,12]

The association indexes (n) obtained for A−O−T−A and A−T−O−T−A were 1.10 ± 0.03 and 1.14 ± 0.04, respectively, at a concentration of 50 mM. These results indicate that the behavior of these systems contrasts with that of their simpler relative A−O−A (n = 1.39 ± 0.04, 25 mM). We conclude that the extent of aggregation (intermolecular association) is less for A−O−T−A and

(12) Schall, O. F.; Robinson, K.; Atwood, J. L.; Gokel, G. W. *J. Am. Chem. Soc.* **1993**, *115*, 5962.

Table 1. Solvent and Salt Dependence of Resonance Positions in A−O−T−A and A−T−O−T−A

	$CDCl_3$[a]				CD_3CN[a]			
compd	T(C6-H)	$T(CH_2)$	A(C8-H)[b]	N-H's	T(C6-H)	$T(CH_2)$	A(C8-H)[b]	N-H's
TOT	7.178	3.780	−	8.224	7.273	3.694	−	9.050
AOA	−	−	7.950	5.610	−	−	7.929	5.876
AOTA	6.941	∼3.4	7.629	6.462	7.119	∼3.4	7.806	6.457
				6.795				6.542
AOTA[c]	6.951	∼3.4	7.641	6.631	−	−	−	−
				6.818				
AOTA + $NaBPh_4$	−	−	−	−	7.053	3.445	7.784	6.044
ATOTA	7.058	∼3.4	7.690	6.009	7.163	∼3.4	7.803	6.135

[a] Concentrations are 5 mM. [b] All C8-H positions in A−O−T−A and A−T−O−T−A refer to the AT side arm. [c] The concentration is 150 mM.

Table 2. Monomer Resonance Positions (ppm) in D_2O Solutions[a]

compd	C6-H	C5-CH_3	T-CH_2	C8-H,C2-H	C8-H,C2−H[c]
A-*n*-Pr[b]	−	−	−	8.130, 8.202	−
T-*n*-Pr[b]	7.500	1.883	3.717	−	−
AOA	−	−	−	8.129, 8.176	−
TOT	7.497	1.883	3.778	−	−
AOTA	7.284	1.735	3.460	8.141, 8.173	8.008, 8.082
ATOTA	7.307	1.720	3.519	−	8.004, 8.084

[a] All solutions were 5 mM using TSP standard as 0.00 ppm. [b] Pr stands for propyl. [c] Refers to proton resonances in the AT side arm.

A−T−O−T−A than for A−O−A, perhaps a result of unfavorable entropy. We infer from the low association index that the chemical shift changes observed in the NMR spectra for the compounds in this study arises from species which are associated largely intramolecularly.

Effects of Solvent Polarity and Metal Cations on the Folded Aggregates. Our intramolecular model notwithstanding, we predicted conformational changes to occur upon increasing the polarity of the medium or upon addition of metal cations. From the data shown in Table 1, it is apparent that the change in solvent from $CDCl_3$ ($\epsilon = 4.8$) to CD_3CN ($\epsilon = 37.5$) diminishes the extent of hydrogen bonding in A−O−T−A (*i.e.* amino resonances shift upfield).

The solvent-induced shifts recorded above contrast with those observed for the T−O−T and A−O−A monomers.[7b] When the solvent was changed from $CDCl_3$ to CD_3CN, downfield shifts of 0.826 and 0.266 ppm, respectively, were noted for these monomers. These changes are presumably due to stronger hydrogen bonding of the monomers to acetonitrile than to chloroform. In A−O−T−A, solvent stabilization of the more compact, stacked side arms may be favored in free energy terms over intramolecular hydrogen bonding. The net result, however, is less shielding and an upfield shift of 0.253 ppm for the more downfield amino resonance (the latter is involved in intramolecular hydrogen bonding).

The change in solvent from $CDCl_3$ to CD_3CN did not affect the upfield amino group (chemical shift change = +0.005 ppm). The proton resonances for hydrogen atoms attached to carbon in both adenine and thymine residues shifted their positions either downfield or upfield suggesting that in A−O−T−A and A−T−O−T−A weakening of intramolecular hydrogen bonding may also bring about readjustments in the stacked AT side arm (see modeling results above). In aqueous solution, nucleotides generally interact by π-stacking rather than H-bonding largely because of their inherent hydrophobicity. We therefore subjected A−O−T−A and A−T−O−T−A to study in D_2O solutions. The data are shown in Table 2. It is evident that compared to the isolated side arms or the simple monomers, some of the A−O−T−A and A−T−O−T−A resonances are shifted upfield. In A−O−T−A, adenine's proton shifts differ substantially from those observed in $CDCl_3$. The upfield shifts of the AT-side arm's carbon-bound protons are especially notable. Similarly, pyrimidine ring protons are shifted upfield.

We have shown in extensive previous work that lariat ether side arms are organized by a macroring-bound cation when one is present.[13] The reaction of A−O−T−A or A−T−O−T−A with either Na^+ or K^+ is expected to reorganize the ring and side arms to establish more favorable cation−metal interactions. Adenine in either side arm is not expected to interact strongly with either cation because nitrogen is a relatively poor donor for alkali metals. Thymine, on the other hand, could serve as a donor by use of the ether or carbonyl oxygen atoms. Molecular models, however, suggest that neither donor atom is sterically accessible.

In the present case, complexation with Na^+ ion results in signal coalescence and an upfield shift of the amino resonances from two resonances at δ 6.457 and 6.542 to a single line at δ 6.044 (Table 3). These changes are expected since intramolecular H-bonding should diminish as side arm separation increases. The C8-H proton resonance in the A side arm is also shifted upfield, presumably because it is more remote from the AT side arm than in the absence of cations. Small downfield shifts (0.012−0.084 ppm) were observed when the counter ion was changed from BPh_4^- to PF_6^-. This suggests the presence of contact or intimate ion pairs since the shielding effect of phenyl in BPh_4^- should be felt only over short distances. If the cation's solvation sphere was satisfied by side arm donor groups, the anion would be more distant.

No dramatic change was observed when Na^+ (diameter = 1.95 Å)[14] was replaced by K^+ (diameter = 2.66 Å), but it is clear from the NMR data that hydrogen bonding is weaker. The reduction in hydrogen bond strength appears to further alter the stacking geometry. This is apparent from the variations observed in resonance positions. The extent of these effects is different for A−O−T−A and A−T−O−T−A, although the trends are similar.

Temperature Dependence of the A−O−T−A Monomer. As was discovered for the related structure A−O−A,[7b] the NH resonances of A−O−T−A can be resolved

(13) (a) Dobler, M. *Ionophores and their structures*; Wiley Interscience: New York, 1981. (b) Gandour, R. D.; Fronczek, F. R.; Gatto, V. J.; Minganti, C.; Schultz, R. A.; White, B. D.; Arnold, K. A.; Mazzocchi, D.; Miller, S. R.; Gokel, G. W. *J. Am. Chem. Soc.* **1986**, *108*, 4078−4088. (c) Arnold, K. A.; Echegoyen, L.; Fronczek, F. R.; Gandour, R. D.; Gatto, V. J.; White, B. D.; Gokel, G. W. *J. Am. Chem. Soc.* **1987**, *109*, 3716−3721.

(14) Shannon, R. D. *Acta Crystallogr. A* **1976**, *A32*, 751.

Table 3. Effect of Added Na^+ or K^+ on A−O−T−A and A−T−O−T−A Solutions[a]

compd[b]	T(C6-H)	C5-CH3	T(CH2)	N-H's	C2-H, C8-H	C2-H, C8-H[c]
AOTA	7.119	1.794	~3.4	6.457 6.542	8.075, 8.105	8.200, 7.806
AOTA + $NaPPh_4$	7.053	1.717	3.445	6.044	8.054, 7.862	8.187, 7.784
AOTA +$NaPF_6$	7.082	1.729	~3.4	6.096	8.055, 7.946	8.187, 7.790
AOTA + KPF_6	7.042	1.682	3.432	5.978	8.039, 7.879	8.208, 7.756
ATOTA	7.163	1.713	~3.4	6.135	−	8.063, 7.803
AOTA + $NaPF_6$	7.065	1.725	3.459	6.083	−	8.068, 7.829
ATOTA + KPF_6	7.082	1.709	~3.4	6.035	−	8.067, 7.818

[a] All solutions were 5 mM in CD_3CN at 25 °C; the 1.930 ppm signal of CD_2HCN was used as internal standard. [b] All salts were dried over P_2O_5 at ambient temperature under vacuum (0.02 torr) for 24 h prior to solution preparation. [c] These positions refer to the AT side arm.

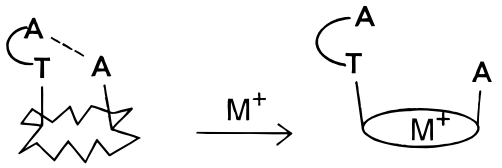

Figure 9. Schematic representation of conformational changes induced by metal cation complexation by A−O−T−A.

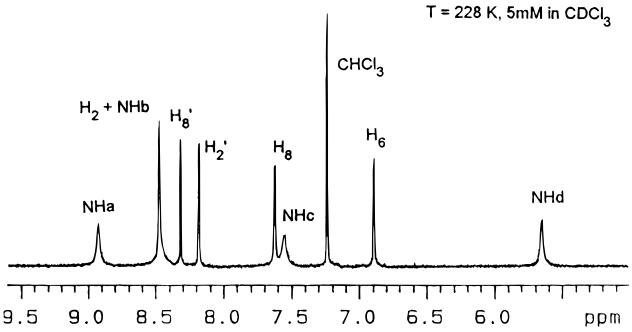

Figure 10. Downfield region of the NMR spectrum of A−O−T−A at −30 °C and a concentration of 5 mM. The peak at δ 7.240 is the signal for nondeuterated solvent ($CHCl_3$).

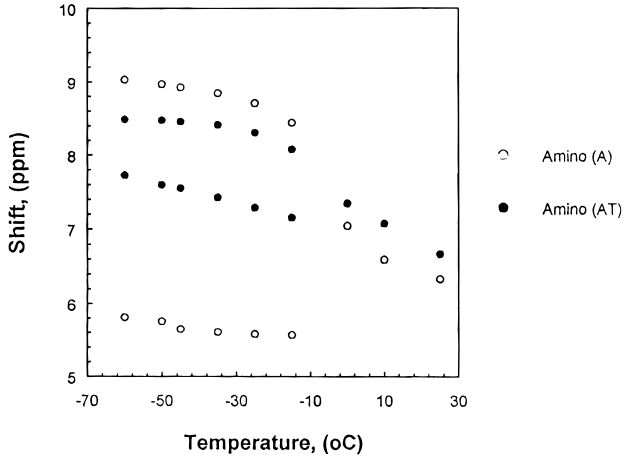

Figure 11. Temperature dependence of the amino resonance hydrogens in A−O−T−A at a concentration of 5 mM in $CDCl_3$.

into four separate signals at low temperature. The temperature effect is dramatic (Figure 10); the downfield signals for A−O−T−A were recorded at −45 °C. The temperature dependence of several of the individual NH resonances are plotted in Figure 11.

Three of the four adenine amino group NH resonances of A−O−T−A are observed as separate signals; Hb and C2H both occur at 8.46 ppm. The ^{1}H-NMR signals for the two hydrogen atoms ($-NH_2$) on the (AT) adenine C6

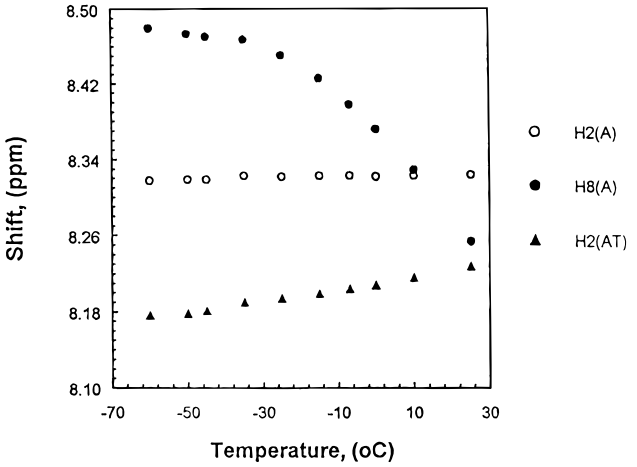

Figure 12. Temperature dependence of the carbon-bound hydrogen resonances in A−O−T−A at a concentration of 5vmM in $CDCl_3$.

are observed at δ 5.651 and 8.927. This signal separation of more than 3 ppm (−60 °C) is made even more remarkable by the fact that the hydrogen atoms are attached to the same nitrogen atom. The splitting point of the signals (see Figure 11) was not observed in this case due to extensive signal broadening in the range −10 → 0 °C but must be *ca.* −5 °C.

The C8-H signal (A side arm) shifted downfield by 0.2 ppm over the +25 → −60 °C temperature range of this study (Figure 12). The decrease in molecular motion as the temperature is lowered may increase the overall stability of the folded aggregates. As intramolecular hydrogen bonding is strengthened, the C8-H in the A side arm should be further deshielded by the AT side arm. It is interesting to note that C2-H in the A side arm, due to its surrounding environment, showed no discernible temperature dependence.

The adenine C2-H (AT side arm) shifted upfield as temperature increased probably due to shielding by the pyrimidine's carbonyl. The C8 proton in this adenine shifted slightly upfield (7.630 → 7.603 ppm) as the temperature was lowered, but at about −15 °C began to move downfield (7.603 → 7.644 ppm). Certain NH proton assignments were made after undertaking the NOE experiments shown in Figure 13. Using the latter information, assignments were made for the resonances whose temperature dependence is shown in Figures 11 and 12 (above). The curves, from top to bottom of that graph correspond to Ha (top), Hb, Hc (intramolecularly hydrogen-bonded), and Hd (bottom). All four resonances were clearly resolved at −35 °C. We could identify the NH involved in intramolecular hydrogen bonding since its resonance position remained unchanged upon dilution

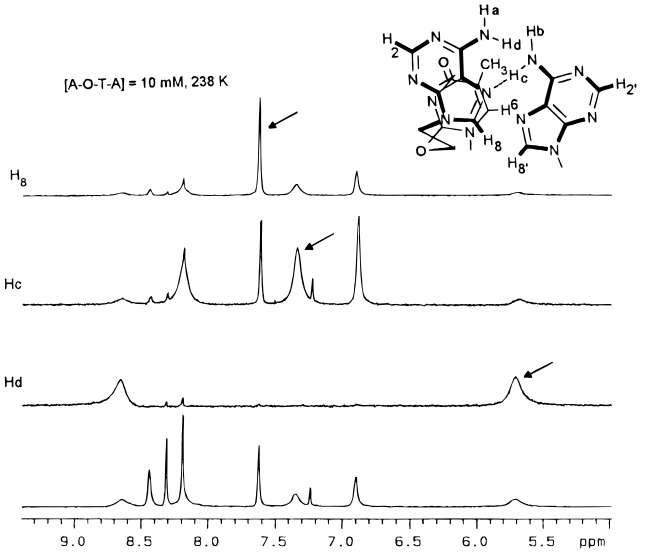

Figure 13. NOE signals produced by selective irradiation of the indicated resonances in A−O−T−A in $CDCl_3$.

from 25 to 5 mM. Selective saturation of Hc (10 mM, −35 °C) caused a considerable decrease in the intensities of Hb, C8-H in the AT side arm, and C6-H in the neighboring pyrimidine ring. Small NOEs to Ha and Hd were also observed.

Saturation of the C8-H (AT side arm) caused a decrease in intensity for C6-H and all four N-H resonances. The decrease in intensity of Hb is due to positional exchange with Hc. The occurrence of these NOEs supports the AT side arm stacking pattern shown in Figure 7 (above). It is interesting to note that saturation of Ha diminishes the signal intensity of Hd as well as the C8-H signal in the A side arm and the C2-H resonances in both side arms. This phenomenon may be due to intermolecular interactions between the aggregates which we have not yet fully defined. When Hd is saturated, an NOE is observed with Ha, the second proton on the same amine nitrogen. No other signal is affected. An H-bond interaction with the adenine amino group (A side arm) was not detected. The fact that Hd is essentially isolated may explain its high field resonance position compared to that of Ha.

Temperature Dependence of the A−T−O−T−A Monomer. In the A−T−O−T−A case, the NH resonances split at a lower temperature (<−20 °C) than observed in A−O−T−A, behavior that is reminiscent of the A−O−A monomer (Figure 14). Only two amino resonances were observed for this symmetrical structure.

Unlike the A−O−T−A monomer, the most downfield NH proton in A−T−O−T−A was observed (−45 °C) at δ 7.363 (compared to δ 8.460 in A−O−T−A). The resonance was concentration dependent (10 → 5 mM, $\Delta\delta$ = +0.014 ppm). The most upfield NH resonance (least H-bonding) had $\Delta\delta$ = +0.043 ppm (same conditions as above). From the smaller dilution effect, we infer that participation of the former amino NH proton in intramolecular H-bonding is greater than is that of the latter. Selective irradiation of the most downfield amino resonance resulted in an intensity decreases for the other NH resonance, for C6-H in the pyrimidine ring, and for the C8-H resonance. A small NOE effect to the C2-H was detected as well. These results suggest that folding of A−T−O−T−A is similar to that in A−O−T−A and that intermolecular association also occurs.

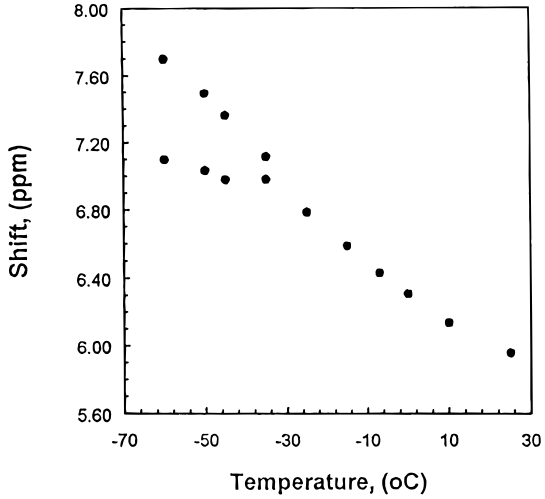

Figure 14. Temperature dependence of the amino hydrogen resonance in A−T−O−T−A at a monomer concentration of 5 mM in $CDCl_3$.

Interplay between Hydrogen Bonding and Stacking Interactions. The adenine amino resonance of A−T−O−T−A appears (in $CDCl_3$) as a broad singlet centered at 6.009 ppm, 0.453 and 0.786 ppm more upfield than those of A−O−T−A, but 0.328 ppm downfield from the corresponding signal observed for A−O−A. In addition, some of the nonexchangeable signals are shifted downfield relative to those of A−O−T−A although they are upfield of those in A−O−A.

Intramolecular hydrogen bonding in A−O−A should be stronger than for A−O−T−A or A−T−O−T−A because the inter-adenine distance as judged from CPK models can be the shortest of the three compounds.[7b] The latter has the potential for the greatest amount of π-stacking since two AT side arms offer the largest overall potential for surface contact among the three compounds.

The evidence we have gathered suggests that hydrogen bonding and π-stacking influence each other. For example, the adenine residues of A−O−T−A are separated by the crown ring and thymine whereas only the macrocycle separates them in A−O−A. Formation of a hydrogen bond between the A−O−T−A side arm leads to a compact structure in which π-stacking is also clearly in evidence. It appears that these two interactions reinforce each other in the A−O−T−A case. A larger stacking potential would be expected in A−T−O−T−A; however, this fact is not evidenced by the NMR data. We interpreted this to mean that H-bonding and π-stacking augment each other in A−O−T−A to give a higher than expected level of overall molecular organization. The NMR data suggest that in this group, molecular organization in A−O−T−A is greater than in either A−O−A or A−T−O−T−A because H-bonding and π-stacking can occur simultaneously in this unique structure.

Biological Significance of Hydrogen Bonding and π-stacking Cooperativity. Single bond interactions between DNA bases have been observed in the solid state structures of tRNAs.[15] In tRNAs, one H-bond may not suffice to secure a particular conformation, but its stabil-

(15) (a) Westhof, E.; Dumas, P. *J. Mol. Biol. J. Mol. Biol.* **1985**, *184*, 119. (b) Kim, S.-H. *Adv. Enzymol.* **1981**, *46*, 279. (c) Jack, A.; Ladner, J. E.; Klug, A. *J. Mol. Biol.* **1976**, *108*, 619.

ity is augmented by π-stacking with neighboring bases. The latter has been shown to involve single base intercalation.[2,15] Although adenine−adenine base-pairing involving two hydrogen bonds has been observed experimentally,[6,16] the two compounds of the present study demonstrate that, when favored, interactions involving a single hydrogen bond are indeed possible in less complex systems, and that feeble forces such as π-stacking and hydrogen bonding may modulate one another.

The existence of interactions similar to those invoked here has been suggested to play a decisive role in recognition and transport processes involving synthetic and biological systems.[17−19] The 5′-termini of most eukaryotic mRNAs consist of a *cap* structure characterized by the presence of a 7-methylguanosine residue. Ueda *et al.*[18] have proposed a cooperative binding mode involved in the recognition of this *cap* structure by a translation initiation factor or cap binding protein (CBP). The latter study considered molecular models of specific sequences present at the protein's probable binding site. Their findings, based upon binding constant determinations, suggested that stacking between a tryptophan and the methylated guanine strengthened pairing by two hydrogen bonds between the latter and a glutamic acid side chain two residues away.

A comparable binding interplay may exist in the recognition of guanine-containing nucleosides by the enzyme ribonuclease T1.[19] From the X-ray structure analysis, the tyrosine residue is found to be about 3.5 Å above the base's plane (see schematic in Figure 15). The electron density map shows a neighboring portion of weak electron density. From the observations, the authors inferred that a conformational change of the enzyme is probable when substrate binding occurs. It was postulated that the tyrosine residue could swing over and stack upon guanine therefore stabilizing hydrogen bonds to the main chains of two aspartamine residues.

The effect of a metal cation on noncovalent interactions and structure was also explored. A−O−T−A and A−T−O−T−A reflect conformational changes induced by cation binding which may be similar to those brought about by cation modulation of phosphate−phosphate repulsions in nucleic acid strands.

The results presented herein demonstrate that noncovalent interplay motifs believed to occur in more complex biological systems may be conveniently reproduced and studied within more readily accesible and modest molecular frameworks.

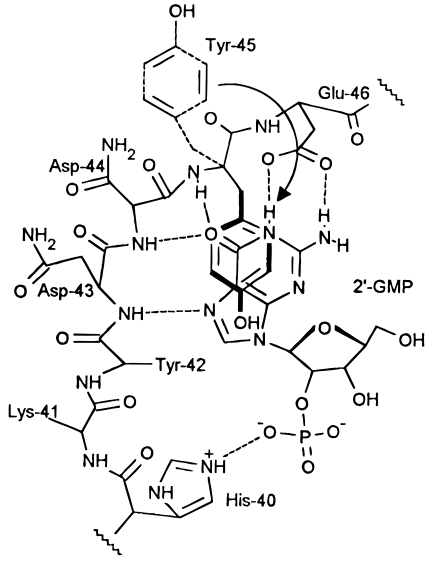

Figure 15. Schematic representation of GMP recognition by the enzyme ribonuclease T1.

Conclusion

Taken together, the data presented here suggest that intramolecular H-bonding and π-stacking diminish in this series of compounds: A−O−T−A > A−T−O−T−A > A−O−A. The greatest conformational stability in this group is exhibited by A−O−T−A because the interplay of side arm H-bonding and π-stacking is the most favorable in the group. Such interactions are also possible in A−T−O−T−A but are diminished relative to A−O−T−A by variations in distances between the side arm elements. The relative simplicity of these model molecules compared to far more complex biological structures facilitates the study of noncovalent interactions at a level not accessible before and allows one to observe how these interactions are affected by changes within the molecule and in the surrounding environment.

Experimental Section

NMR spectra (1D), one-dimensional NOE, two-dimensional correlated (2D-COSY), and phase-sensitive nuclear Overhauser enhancement (NOESY) spectra were recorded at 400 MHz unless otherwise specified. Chemical shifts were reproducible within a ±0.002 ppm range. $CDCl_3$ was used as solvent, unless otherwise specified. Chemical shifts are given in ppm (δ) downfield from DSS (for D_2O solutions), or from residual, nondeuterated, solvent ($CHCl_3$, δ 7.240; CD_3SOCD_2H, δ 2.490; or HCD_2CN, δ 1.930) as reference. NOESY spectra were determined using a mixing time of 0.6 s. The time domain data sets were accumulated over a sweep width of 3042 Hz using 1024 complex data points in the t2 dimension. The repetition delay was 1.0 s and 68 scans were collected for each t1 increment (512 total). COSY spectra were accumulated over a sweep width of 3013 Hz using 1024 complex data points in the t2 dimension. Eighty-eight scans were collected for each t1 increment (512 total). Two-dimensional data sets were processed using instrument software. Infrared (IR) spectra were recorded on KBr disks and are reported in cm^{-1}, calibrated against the 1601 cm^{-1} band of polystyrene. DCI mass spectra were determined using methane or ammonia as the carrier gas (DCI) and are reported as m/z (%FS). Vapor pressure osmometry experiments were carried out using previously described procedures.[7b,12] Melting points were determined on a capillary melting point apparatus and are uncorrected. Combustion analyses were performed by Atlantic Microlab, Inc., Atlanta, GA. TLC analyses were performed on aluminum oxide 60 F-254, neutral (type E), or on silica gel

(16) (a) Westhof, E.; Sundaralingam, M. *Proc. Natl. Acad. Sci. U.S.A.* **1980**, *77*, 1852. (b) Maskos, K.; Gunn, B. M.; LeBlanc, D. A.; Morden, K. M. *Biochemistry* **1993**, *32*, 3583. (c) Eschenmoser. A. *Helv. Chim. Acta* **1993**, *76*, 259 and 2161. (d) Seela, F.; Winter, H. *Helv. Chim. Acta* **1994**, *77*, 597.

(17) (a) Constant, J. F.; Fahy, J.; L'homme, J. *Tetrahedron Lett.* **1987**, 1777. (b) Sheridan, R. E.; Whitlock, H. W., Jr. *J. Am. Chem. Soc.* **1986**, *108*, 7120. (c) Saito, I.; Sugiyama, H.; Matsuura, T.; Keiichi, F. *Tetrahedron Lett.* **1985**, *4467*. (d) Sessler, J. L.; Furuta, H.; Kral, V. *Supramol. Chem.* **1993**, *1*, 209. (e) Kral, V.; Sessler, J. L. *Tetrahedron* **1995**, *51*, 539.

(18) (a) Ueda, H.; Doi, M.; Inoue, M.; Ishida, T.; Tanaka, T.; Uesugi, S. *Biochem. Biophys. Res. Commun.* **1988**, *154*, 199. (b) Ueda, H.; Iyo, H.; Doi, M.; Inoue, M.; Ishida, T. *Biochim. Biophys. Acta* **1991**, *1075*, 181. (c) Tarui, M.; Furumuna, H.; Kafuku, Y.; Ishida, T.; Inoue, M. *Biochem. Biophys. Res. Commun.* **1992**, *183*, 577. (d) Ishida, T.; Tarui, M.; In, Y.; Ogiyama, M.; Doi, M.; Inoue, M. *FEBS Lett.* **1993**, *333*, 214. (e) Ishida, T.; Toda, Y.; Tarui, M.; Doi, M.; Inoue, M. *Chem. Pharm. Bull.* **1994**, *42*, 674.

(19) (a) Heinemann, U.; Saenger, W. *Nature* **1982**, *299*, 27. (b) Arni, R.; Heinemann, U.; Tokuoka, R.; Saenger, W. *J. Biol. Chem.* **1988**, *263*, 15358.

60 F-254. Preparative chromatographic columns were packed with aluminum oxide (50 g per gram of sample, activated, neutral, Brockmann 150 mesh), standard grade. Centrifugally accelerated PTLC was performed using 2 and 4 mm layer thickness circular plates, coated with either aluminum oxide GF or silica gel GF. All reactions were conducted under an atmosphere of dry N_2. Acetonitrile was dried and distilled over CaH_2. Dry solvents were stored over activated molecular sieves (3 Å). All other solvents and reagents were of the best grade available commercially and were used without further purification, unless otherwise stated.

NMR Sample Preparation. All glassware was dried in an electric oven at 110 °C overnight. All glassware, equipment, and volumetric flasks containing powder samples were introduced in a desiccator and left *in vacuo* (≤0.1 torr), over P_2O_5, for at least 12 h prior to sample preparation. All solutions were prepared and transferred in a glove bag under an atmosphere of dry argon, in the presence of P_2O_5 as desiccant. All deuterated solvents were dispensed from sealed ampoules and were of the highest purity available commercially. Water contents in samples prepared under such conditions were typically $\sim 2.5 \times 10^{-4}$ M, as judged from integrals of ^{1}H-NMR signals.

Variable Temperature Experiments. These experiments were conducted under instrument control and the temperature was controlled to within a ±0.2 °C range.

Molecular Modeling Simulations. The structure of A−O−T−A was constructed using version 6.0 of SYBYL. Atomic charges were calculated using the Gasteiger-Huckel model. Structures were minimized and interaction energies calculated using the Powell method and the Tripos force field (500 iterations, dielectric constant = 4.8).

***N*-(3-Thymin-1-ylpropyl)-4,13-diaza-18-crown-6, T−O.** 4,13-Diaza-18-crown-6 (2.0 g, 7.6 mmol), 1-(3-chloropropyl)-thymine[7b,20] (1.88 g, 7.6 mmol), and Na_2CO_3 (1.62 g, 15.2 mmol) were stirred at room temperature in CH_3CN (30 mL) for 8 d. The reaction was filtered and the solvent removed *in vacuo*. Column chromatography (Al_2O_3, 0−3% MeOH:$CHCl_3$) afforded fractions which yielded the product as a thick slightly yellow oil. Crystallization from EtOAc afforded T−O as slightly yellow crystals (40%, mp 111−112 °C). ^{1}H-NMR: δ 1.813 (m, 2H, $CH_2CH_2CH_2$), 1.913 (s, 3H, CH_3), 2.528 (t, 2H, N[crown]-CH_2), 2.721 (t, 4H, CH_2NCH_2, unsubstd side), 2.773 (t, 4H, CH_2NCH_2, substd side), 3.616 (m, 17H, $CH_2O(CH_2)_2OCH_2$ + NH), 3.830 (t, 2H, thy-CH_2), 7.280 (s, 1H, C6-H), 9.05 (broad s, 1H, imide-H, exchanged in D_2O). IR: 3650−3200 (br), 2860, 1930, 1660, 1435, 1350, 1275, 1220, 1175, 1100, 1065, 1040, 1000, 945, 885, 805, 765, 735, 680, 645 cm^{-1}. Anal. Calcd for $C_{20}H_{36}N_4O_6$: C, 56.06; H, 8.47; N, 13.07%. Found: C, 55.88; H, 8.40; N, 13.00%.

***N′*-(2-Adenin-9-ylethyl-*N*-{3-[*O*^{2}-(2-adenin-9-ylethyl)-thymin-1-yl]propyl}-4,13-diaza-18-crown-6, A−O−T−A.** 9-(2-Chloroethyl)adenine[7b,21] (0.265 g, 1.34 mmol) and T−O (0.15 g, 0.35 mmol) were dissolved in *n*-PrCN (10 mL). To the clear solution were added Na_2CO_3 (0.21 g, 2.04 mmol) and NaI (0.011 mg, 0.07 mmol). The resulting suspension was stirred at reflux for 72 h. After this time, all T−O had been consumed, although some of the adenine analog was still present (TLC). The reaction was cooled to room temperature and filtered. The solvent was removed *in vacuo* affording a thick, light brown oil. A combination of column chromatography (Al_2O_3, 0−3% MeOH:$CHCl_3$), and centrifugally accelerated PTLC (Al_2O_3 rotor, 2−4% MeOH:CH_2Cl_2) was utilized for isolating the major product. The product was obtained as a white foam (165 mg, 55% from T−O). Analytically pure material was isolated after slow crystallization from MeCN (over 10 days, ~60 mL/g) as a white amorphous solid (mp 136−138 °C). ^{1}H-NMR (5 mM): δ 1.444 (m, 2H, $CH_2CH_2CH_2$); 1.888 (s, 3H, Thy-CH_3); 2.352 (t, 2H, thy-$CH_2CH_2CH_2$); 2.688 (t, 4H, CH_2NCH_2, in AT side arm side); 2.728 (t, 4H, CH_2NCH_2, in A side arm side); 2.851 (t, 2H, ade′-CH_2CH_2); 3.365, (t, 4H, OCH_2CH_2N, in AT side arm side); 3.490 (m, 6H, OCH_2CH_2N, in A side arm side + thy-CH_2); 3.553 (m, 8H, OCH_2CH_2O); 4.216 (t, 2H, ade′-CH_2); 4.404 (t, 2H, ade-CH_2); 4.519 (t, 2H, thy-OCH_2), 6.462 (broad s, 2H, NH_2, exchanged in D_2O); 6.795 (broad s, 2H, NH_2, exchanged in D_2O); 6.941 (s, 1H, Thy C6-H); 7.629 (s, 1H, Ade C8-H); 8.221 (s, 1H, ade′ C2-H); 8.263 (s, 1H, ade′ C8-H); 8.316 (s, 1H, ade C2-H). IR: 3330 (br), 3180 (br), 2380, 1620, 1590, 1450, 1410, 1350, 1295, 1250, 1205, 1105, 1070, 905, 800, 770, 725, 645 cm^{-1}. MS (DCI) 751 (10), 424 (27), 288 (30), 179 (12), 162 (45), 152 (25), 136 (100). Anal. Calcd for $C_{34}H_{50}N_{59}O_6$, C 54.36; H, 6.71; N, 26.12%. Found: C, 54.29; H, 6.74; N, 26.09%.

The $NaBPh_4$ complex was isolated after treating A−O−T−A (150 mg, 0.21 mmol) with sodium tetraphenylborate (74.3 mg, 0.21 mmol). The solids were dissolved in $CHCl_3$:acetone (1:1, 25 mL) and stirred for 30 min. The solvents were removed *in vacuo*, and the resulting foam was dissolved, at reflux, in a minimum amount of the same solvent mixture. A white solid was collected upon cooling (200 mg, 92%, mp 115−120 °C). ^{1}H-NMR (MeCN-d_3): δ 1.539 (m, 2H, $CH_2CH_2CH_2$), 1.717 (s, 3H, thy-CH_3), 2.163 (s, 2H, H_2O), 2.279 (t, 2H, thy-CH_2-CH_2CH_2), 2.574 (t, 4H, CH_2NCH_2, in AT side arm side), 2.695 (t, 2H, CH_2NCH_2, in A side arm side), 2.940 (t, 2H, ade′-CH_2CH_2), 3.441 (t, 2H, thy-CH_2), 3.531 (m, 16H, CH_2OCH_2-OCH_2), 4.196 (m, 4H, ade′-CH_2 + ade-CH_2), 4.380 (t, 2H, thy-OCH_2 6.044 (broad s, 4H, NH_2, exchanged in D_2O), 6.831 (t, 4H, C4-H in phenylborate), 6.983 (t, 8H, C3,5−H in tetraphenylborate), 7.052 (s, 1H, thy C6-H), 7.261 (broad s, 8H, C2,6-H in phenylborate), 7.784 (s, 1H, ade C8-H), 7.862 (s, 1H, ade′ C8-H), 8.054 (s, 1H, ade′ C2-H), 8.187 (s, 1H, ade C2-H). IR: 3690−2800 (br), 1620, 1460, 1415, 1350, 1325, 1295, 1240, 1205, 1175, 1095, 1030, 1000, 930, 905, 840, 795, 765, 730, 700, 645 cm^{-1}. Anal. Calcd for $C_{58}H_{70}N_{14}O_6BNa\cdot H_2O$: C, 62.70; H, 6.53; N, 17.64%. Found: C, 62.87; H, 6.51; N, 17.58%.

***N,N′*-Bis{3-[*O*^{2}-2-adenin-9-ylethyl)thymin-1-yl]propyl}-4,13-diaza-18-crown-6, A−T−O−T−A** was prepared as described above for A−O−T−A. T−O−T (400 mg, 0.676 mmol), 9-(2-chloroethyl)adenine (300 mg, 1.49 mmol), Na_2CO_3 (700 mg, 5.8 mmol), and NaI (100 mg, 0.52 mmol) were refluxed in *n*-PrCN (11 mL) for 72 h. Column chromatography (Al_2O_3, 2−4% MeOH:$CHCl_3$) and centrifugally accelerated PTLC (Al_2O_3 rotor, 5% MeOH:$CHCl_3$) afforded the product as a foamy white solid. The foam was crystallized from water (≈10 mL/g). The product was obtained as colorless crystals (520 mg, 85%, turn opaque when dry, mp 113−116 °C). ^{1}H-NMR: δ 1.567 (t, 4H, $CH_2CH_2CH_2$), 1.831 (s, 6H, thy-CH_3), 1.957 (s, 3H, H_2O, exchanged in D_2O), 2.382 (t, 4H, N[crown]-CH_2), 2.673 (t, 8H, CH_2NCH_2 in crown), 3.545 (t, 8H, NCH_2CH_2O), 3.601 (s, 8H, OCH_2CH_2O), 4.401 (t, 4H, Ade-CH_2), 4.508 (t, 4H, thy-OCH_2), 6.009 (broad s, 4H, NH_2, exchanged in D_2O), 7.058 (s, 2H, thy C6-H), 7.690 (s, 2H, ade C8-H), 8.230 (s, 2H, ade C2-H). IR: 3600−3000 (br), 2950, 2880, 1610, 1460, 1350, 1310, 1250, 1215, 1125, 1105, 1080, 1020, 945, 920, 860, 800, 770, 720, 655 cm^{-1}. Anal. Calcd for: $C_{42}H_{64}N_{16}O_8\cdot 1.5H_2O$: C, 53.44; H, 6.73; N, 23.64%. Found: C, 53.45; H, 6.73; N, 23.66%.

Acknowledgment. We thank the NIH for a grant (GM 36262) that supported this work.

JO951959L

(20) (a) Leonard, N. J.; Scott, T. G.; Huang, P. C. *J. Am. Chem. Soc.* **1967**, *89*, 7137. (b) Brown, D. T. In *Synthetic Procedures in Nucleic Acid Chemistry*; J. Wiley & Sons: New York, 1969; Vol. 1, pp 96−97.

(21) Brown, D. T. In *Synthetic Procedures in Nucleic Acid Chemistry*; J. Wiley & Sons: New York, 1969; Vol. 1, pp 3−5.